

## Sinuosity of Martian rampart ejecta deposits

Nadine G. Barlow

Lunar and Planetary Institute, Houston, Texas

**Abstract.** The sinuosities of 2213 Martian rampart ejecta craters are quantified through measurement of the ejecta flow front perimeter and ejecta area. This quantity, called lobateness, was computed for each complete lobe of the 1582 single lobe (SL), 251 double lobe (DL), and 380 multiple lobe (ML) craters included in this study. A lobateness value of 1 indicates a circular ejecta blanket, whereas more sinuous ejecta perimeters have lobateness values  $>1$ . Although resolution does have an effect on the absolute values of lobateness, the general relationships between lobateness and morphology exist regardless of resolution. Evaluation of the lobateness values reveals that the outer lobes of DL and ML craters have higher median lobateness values (i.e., are more sinuous) than the inner lobes. The outermost lobe of ML craters displays higher lobateness values than the outer lobe of DL craters or the single lobe of SL craters. Previous reports of lobateness-diameter, lobateness-latitude, and lobateness-terrain relationships for rampart craters are not supported by this study. Many of the differences between the results of this study and the previous lobateness analyses can be attributed to the inclusion of resolution effects and the distinction between different ejecta morphologies in this study. The results of this study taken together with a previous analysis of the distribution and diameter dependence of different ejecta morphologies are most consistent with the theory that Martian lobate ejecta morphologies form from impact into subsurface volatiles.

### Introduction

The lobate ejecta morphology associated with Martian impact craters is distinctly different from the ballistically emplaced ejecta surrounding lunar and Mercurian craters. The rampart morphology, characterized by fluidized ejecta terminated by a distal ridge, is the most common of the Martian ejecta morphologies. Two theories have been proposed to explain the formation of the rampart morphology. The first proposes that vaporization of subsurface volatiles results in flow emplacement of the ejecta [Carr *et al.*, 1977; Gault and Greeley, 1978; Greeley *et al.*, 1980; Kieffer and Simond, 1980]. The second theory suggests that atmospheric gases provide the fluidizing medium which incorporates the ejected material of a particular size range [Schultz and Gault, 1979, 1982, 1984; Schultz, 1992]. Both theories adequately describe many of the qualitative aspects of the lobate ejecta morphologies, but few quantitative studies of morphologic characteristics currently exist. This study expands the amount of quantitative data for rampart craters by measuring the sinuosity of the fluidized ejecta blankets. Taken alone, the results do not uniquely distinguish between the two formation theories outlined above, but do provide new insights into the similarities and differences between the various ejecta morphologies.

Qualitative studies of ejecta morphology and mobility have been interpreted in terms of impact into ice versus impact into fluid reservoirs [Johansen, 1978, 1979; Mougins-Mark, 1979, 1981; Blasius and Cutts, 1981; Horner and Greeley, 1987; Barlow and Bradley, 1990; Costard, 1989; Kargel, 1989]. Kargel [1986] was the first to quantify ejecta sinuosity by developing a formula for "lobateness" of the ejecta:

$$\Gamma = P/(4\pi A)^{1/2} \quad (1)$$

where  $\Gamma$  is the lobateness,  $P$  is the perimeter of the lobate ejecta blanket, and  $A$  is the area covered by the ejecta blanket. (Note that in later studies [Kargel, 1989; Baker *et al.*, 1993], the above formula has 1 subtracted from it, resulting in  $\Gamma$  values  $\geq 0$ .) Using equation (1), a circular ejecta deposit has a  $\Gamma$  of 1 while more sinuous deposits have  $\Gamma > 1$ . Kargel [1986] initially computed lobateness values for 538 rampart craters located in selected areas of Mars (Figure 1). Approximately one-fourth of the craters in his analysis are located on heavily cratered units of the southern highlands; the remainder are found on moderately to lightly cratered plains units of various ages. The results of Kargel's study suggested that  $\Gamma$  depends on crater size at low latitudes; larger craters displayed higher  $\Gamma$  values than smaller crater within the equatorial regions of Mars. Kargel followed Johansen's [1979] interpretation that less sinuous ejecta resulted from impact into ice and craters with higher  $\Gamma$  owed their flower-like appearance to impact into water. Kargel further argued that water reservoirs lay beneath a near-surface ice-rich permafrost layer and that larger craters have higher  $\Gamma$  values because they excavate into this water-rich region. Kargel found no indication of a relationship between  $\Gamma$  and elevation or geologic unit, although a later study of 650 craters with a more global distribution reports a hemispheric asymmetry in lobateness as well as ejecta extent [Kargel, 1989].

Evaluation of Kargel's study led us to conclude that the quantification of sinuosity in terms of the lobateness value may hold information useful to the further understanding of fluidized ejecta morphologies on Mars and their possible origin(s). We therefore have undertaken an expanded lobateness study of lobate ejecta morphologies on Mars by (1) increasing the number of craters in the study, (2) expanding the study to a global distribution of rampart craters, thereby increasing the number of geologic units studied, (3) distinguishing between different ram-

Copyright 1994 by the American Geophysical Union.

Paper number 94JE00636.  
0148-0227/94/94JE-00636\$05.00

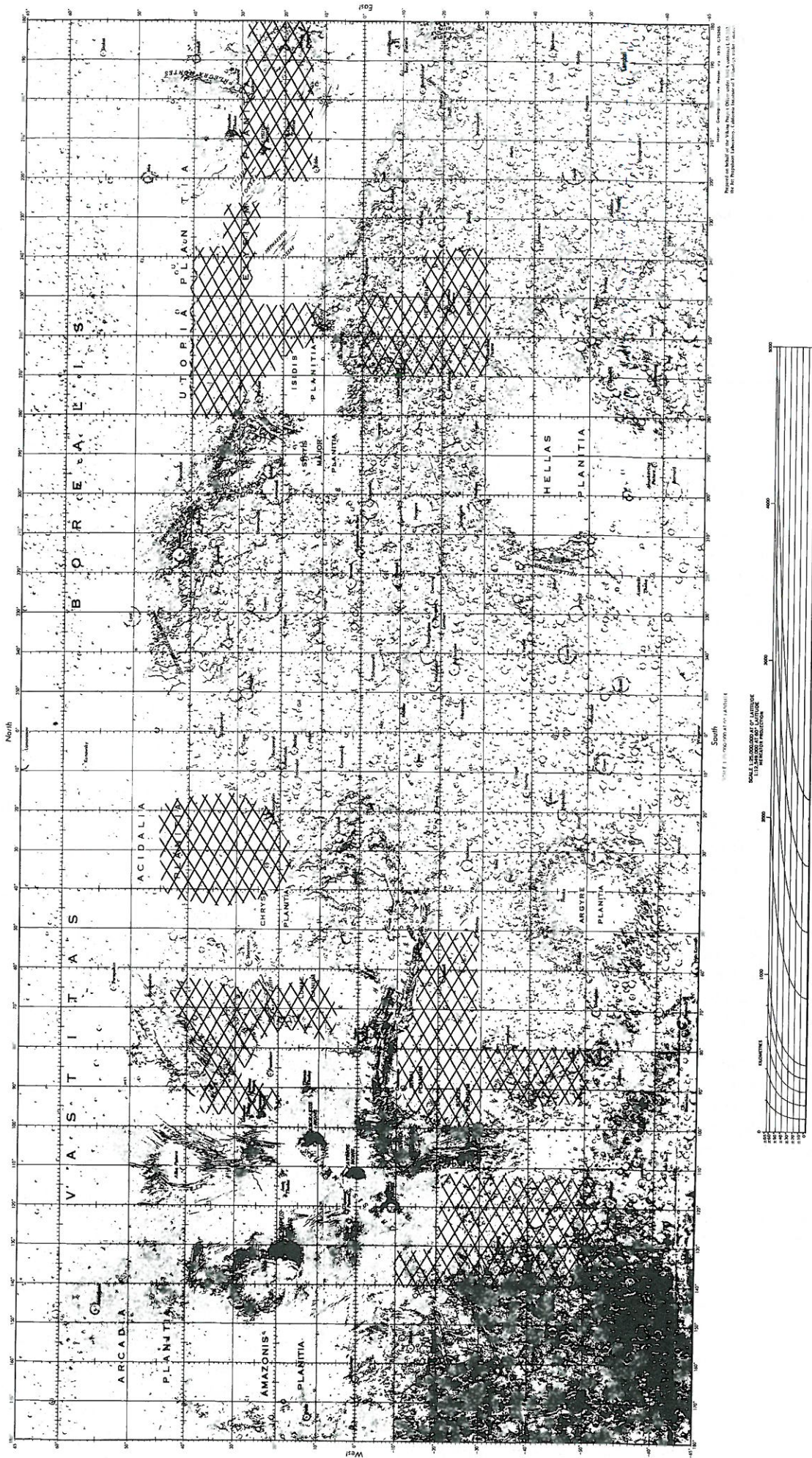


Figure 1. Distribution of rampart craters used in the lobateness study by Kargel [1986]. The cross-hatched areas show the regions of major concentration of the craters used in the study.

part ejecta morphologies, and (4) computing lobateness values for all ejecta lobes which can be distinguished as extending completely around the crater. In addition, we have studied the effects of image resolution on the results of the lobateness analysis to determine which correlations are real and which are simply the result of resolution.

This study utilizes 1582 single-lobe (SL) craters, 251 double-lobe (DL) craters, and 380 multiple-lobe (ML) craters distributed across the entire Martian surface and exhibiting crater diameters between 8 and 80 km. Ejecta lobes were traced from Viking 1:2M photomosaics (resolutions commonly between 130 and 300 m/pixel), and from higher-resolution Viking images (resolutions between 40 and 150 m/pixel) for selected images. Ejecta perimeters and areas were measured using a digitizing table and the corresponding lobateness was computed using equation (1).

Correlations between diameter and lobateness for each of the three rampart morphologies were analyzed using  $\sqrt{2}$  diameter increments (as recommended by the *Crater Analysis Techniques Working Group* [1978]). The frequency of craters decreases with increasing diameter; therefore use of the  $\sqrt{2}$  diameter increments decreases the uncertainty by increasing the size of the diameter ranges (and thus increasing the number of craters) for larger crater diameters. Latitude-lobateness correlations utilized  $10^\circ$  latitude bins, and analysis of geologic units used three generalized categories based on crater statistical ages derived by *Barlow* [1988].

This study finds that image resolution does play a role in the actual lobateness values computed, but comparisons of results between ejecta blankets at similar resolutions indicate that the results detailed below are valid. The analysis reveals no correlation between lobateness and diameter within a specific ejecta morphology class, although diameter is correlated with the different ejecta morphologies (single-lobe and double-lobe morphologies are generally associated with smaller craters than is the multiple-lobe morphology [Barlow and Bradley, 1990]). No correlation between latitude and lobateness for single-lobe or multiple-lobe craters is found. Double-lobe craters are located within very specific latitude ranges and therefore analyses of lobateness variations with changes in latitude and geologic unit are not possible. No statistically significant correspondence between lobateness and geologic unit was found for single-lobe or multiple-lobe craters. In addition, the inner lobe(s) of double- and multiple-lobe craters consistently display lower lobateness values than the outer lobe(s). These results can be reconciled with formation of rampart ejecta blankets either by impact into subsurface volatiles (where differences in ejecta lobe sinuosity are proposed to result from differences in amounts and/or physical states of volatiles) or by interaction with the atmosphere (where sinuosity differences result from changes in the energy of impact). However, the results from this analysis taken together with the *Barlow and Bradley* [1990] study are most consistent with formation of the fluidized ejecta morphologies by impact into and vaporization of subsurface volatiles [Carr et al., 1977].

## Detailed Methodology and Results

Data for this study were obtained from N. G. Barlow (Catalog of large Martian impact craters, submitted to NASA 1994; hereafter referred to simply as the Catalog). The Catalog consists of information on the size, location, regional geologic province, ejecta and interior morphology, and preservational state of 42,283 craters located across the entire Martian surface. Craters range in diameter from 2 to 2000 km, but the Catalog is considered complete for craters  $\geq 8$  km in diameter (25,826 craters).

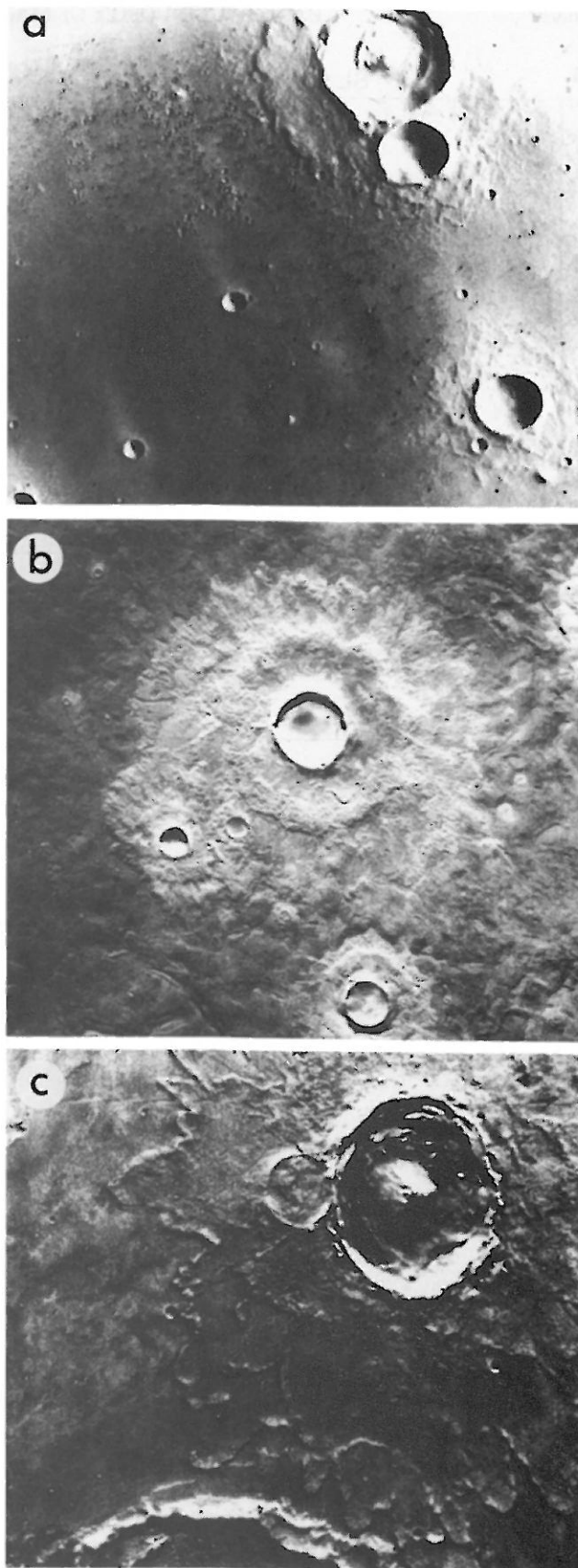


**Figure 2.** Examples of the three rampart ejecta morphologies used in this study. (a) The three largest craters in this image all display a single-lobe ejecta morphology. The largest crater is 10.4 km in diameter (Viking Orbiter frame 004A32). (b) The largest double-lobe crater in this image is 14.5 km in diameter (Viking Orbiter frame 010B81). (c) The multiple-lobe crater Yuty is 18 km in diameter (Viking Orbiter frame 003A07).

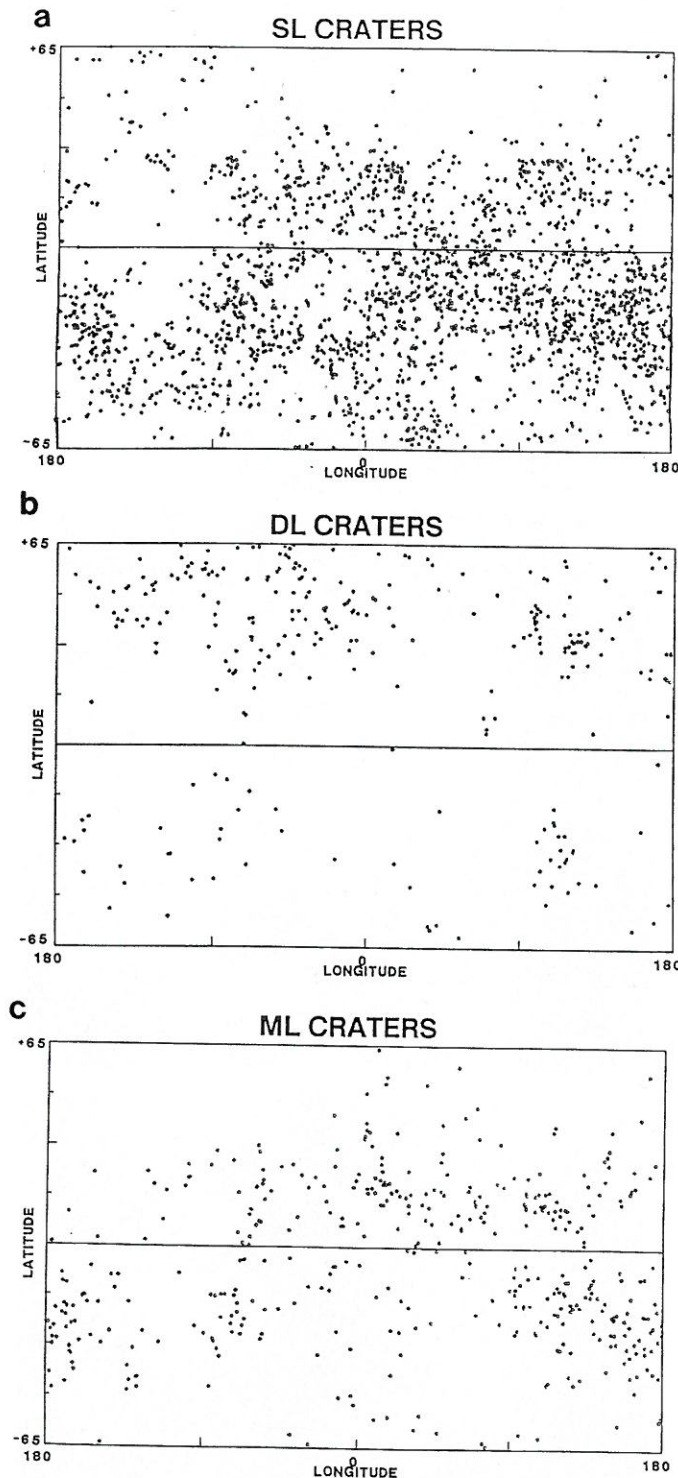


Figure 3. Distribution of (a) single-lobe, (b) double-lobe, and (c) multiple-lobe craters used in this lobateness study.

Craters identified as exhibiting a rampart ejecta morphology (i.e., single-lobe, double-lobe, or multiple-lobe, following the classification system of *Mouginis-Mark* [1979]) were used in this computation of lobateness values (Figure 2). Figure 3 shows the planetwide distribution of the rampart craters used in this analysis. The ejecta perimeters and areas of 1582 single-lobe craters, 251 double-lobe craters, and 380 multiple-lobe craters were measured and lobateness values were computed for

each of these 2213 rampart craters. We believe this fourfold increase in the number of craters over that of *Kargel's* [1986] study is sufficient to give statistically valid results of lobateness variations on the global scale.

The Viking 1:2M photomosaics were used to map the distribution of most ejecta lobe(s) surrounding craters identified with a rampart structure in the Catalog. Ejecta blankets were traced from the photomosaic for each rampart crater utilized in this study and perimeters and areas were determined using a digitizing tablet. The measured ejecta perimeter and area for each complete ejecta blanket were used in equation (1) for computation of the corresponding lobateness value(s). Double-lobe craters have  $\Gamma$  values for both inner and outer ejecta lobes while multiple-lobe craters generally have three distinct lobes for which lobateness values could be computed. Higher-resolution Viking Orbiter frames (40-150 m/pixel resolution) were used to confirm lobateness values for a randomly selected subset of 100 rampart craters. We found that image resolution can affect the measured lobateness value by up to  $\pm 0.15$ , with higher-resolution measurement producing larger lobateness values than measurements made using low-resolution images. However, when resolution is held approximately constant, the relationships noted in subsequent sections were observed.

Most craters for which lobateness values were computed lie within the  $\pm 60^\circ$  latitude range; this range was subdivided into  $10^\circ$  segments for our analysis of latitude-lobateness correlations. Crater diameter-lobateness correlations were studied using  $\sqrt{2}$  diameter increments for all rampart craters between 8 and 80 km. To provide statistically viable results, the geologic unit analysis was generalized to three categories based on a previously reported crater statistical analysis by *Barlow* [1988]: heavily cratered highlands, moderately cratered plains, and lightly cratered plains. Crater size-frequency distribution analyses indicate that the highlands date from the late heavy bombardment period (Noachian), the moderately cratered ridged plains formed near the end of heavy bombardment (Lower Hesperian, or about  $3.8 \times 10^9$  years ago, if the lunar cratering chronology can be directly extrapolated to Mars [*Neukum and Hiller*, 1981]), and the lightly cratered plains have formed since the end of the heavy bombardment period (Upper Hesperian to Upper Amazonian) [*Tanaka*, 1986; *Barlow*, 1988].

#### Single-Lobe Craters

Single-lobe rampart ejecta craters are the most abundant ejecta morphology on Mars, constituting 50.9% of the ejecta blanket classes surveyed by *Barlow and Bradley* [1990] and 85.5% of all rampart crater classes. In this study, lobateness values for 1582 SL craters ranging in diameter from 8 to 33 km were computed and analyzed.

Lobateness values determined using the 1:2M photomosaics (resolutions ranging from 130 to 300 m/pixel) show little change with diameter among SL craters (Figure 4). The lower lobateness values for craters in the 8- to 13-km diameter range is a result of resolution effects, since measurement of lobateness for a subset of craters in this size range using higher-resolution images (40-150 m/pixel) reveals no statistically significant variation in lobateness values among all diameter ranges.

We divided Mars into  $10^\circ$  latitude bins between  $\pm 60^\circ$  latitude and computed the median lobateness within each latitude range (Table 1; Figure 5). We found no significant latitudinal trends in either the northern or southern hemisphere for SL craters. The peak lobateness range in the  $0^\circ$  to  $-50^\circ$  latitude range

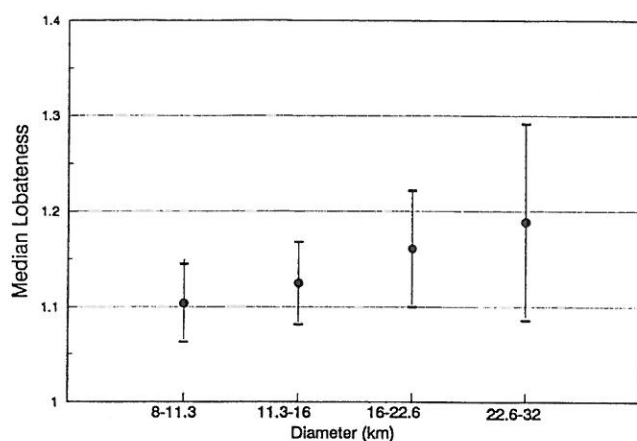


**Figure 4.** Crater diameter versus median lobateness for SL craters using  $\sqrt{2}$  diameter bins. Dispersion of the values is computed from the standard deviation ( $\sigma = \pm\Gamma/\sqrt{N}$ , where  $N$  is the number of craters in the diameter range considered). Within the dispersion limits, no variation in lobateness with increasing crater diameter is observed.

(between 1.1 and 1.2) is slightly higher than that in the  $0^\circ$  to  $+30^\circ$  latitude range (between 1.0 and 1.1), which suggests a slight hemispheric dichotomy, but the standard deviation ( $\sigma = \pm\Gamma/\sqrt{N}$ ) indicates that this difference is not significant at the  $1\sigma$  level.

SL craters superposed on the heavily cratered and moderately cratered terrain units primarily display  $\Gamma$  values between 1.1 and 1.2, while those on lightly cratered units largely have  $\Gamma$  values in the range 1.0 to 1.1 (Table 2). However, the computed uncertainties indicate that this difference is not significant ( $1\sigma$  level).

We also checked for correlations between lobateness and various combinations of latitude, longitude, diameter, and terrain. No correlations between  $\Gamma$  and these combinations are indicated.

#### Double-Lobe Craters

The 251 DL rampart craters utilized in this analysis make up only 6.6% of the ejecta morphologies found across the Martian surface and 11.3% of the rampart morphologies [Barlow and Bradley, 1990]. In this analysis, the lobateness for both the outer and inner lobes of the DL craters was computed. The outer lobe of DL craters generally displays greater lobateness

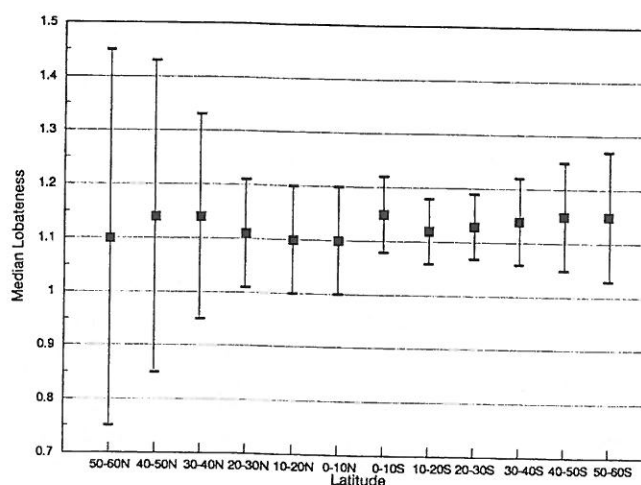


**Figure 5.** Latitude versus median lobateness for SL craters. Dispersion is  $1\sigma$  deviations. No trend between lobateness and latitude is found. See Table 1 for supporting information.

(median  $\Gamma = 1.14$ ) than the inner lobe (median  $\Gamma = 1.09$ ) (Figure 6). We enlarged the inner lobe to the same size as the outer lobe to test resolution effects on this analysis; the inner lobe lobateness increases slightly at higher resolution, but the general relationship of the outer lobe having higher lobateness than the inner lobe is preserved regardless of resolution. A similar result is observed when higher resolution images are used.

The diameter range for DL craters ( $8 \text{ km} \leq D \leq 35 \text{ km}$ ) overlaps with that for SL craters. No strong evidence for any correlation of lobateness with increasing diameter is seen for either the outer (Figure 7) or inner ejecta lobe.

DL craters are found to be concentrated in the  $30^\circ$  to  $50^\circ$  latitude range in both the northern and southern hemispheres (Figure 3b). The limited area extent of DL craters precludes comparative studies of lobateness with latitude or geologic unit. No difference in either peak lobateness range or median  $\Gamma$  is observed for DL craters in the northern hemisphere versus those in the southern hemisphere. In addition, we checked for possible correlations between lobateness and latitude-longitude combinations. As with SL craters, no dependence of  $\Gamma$  on particular latitude-longitude areas is found.

#### Multiple-Lobe Craters

Multiple-lobe rampart craters display a more complex structure than either single or double lobe craters. In addition to having a larger number of surrounding lobes, ML craters also tend to have lobes which do not extend completely around the crater. Since the lobateness formula compares the ejecta perimeter to that of a circle of the same area, we have limited the present analysis to those lobes which extend completely around the crater. Ninety-seven percent of the 380 ML craters in this study have at least two complete lobes, and 50% have at least three lobes. Only six craters (2%) have four complete lobes, the maximum number of complete lobes observed. Table 3 shows that, for the three lobes for which good statistics exist, the median lobateness increases from the inner (median  $\Gamma = 1.09$ ) to the outer lobes (median  $\Gamma = 1.18$ ), although the lobateness is similar for the outer and intermediate lobes. Enlargement of the inner lobes to the same size as the outer lobe as well as use of higher-resolution images again shows that this relationship is real and not a resolution effect. In addition, the lobateness of

**Table 1.** SL Lobateness Versus Latitude

Latitude Range	Number	Minimum $\Gamma$	Maximum $\Gamma$	Median $\Gamma$
50-60°N	10	1.03	3.32	1.10
40-50°N	15	1.01	3.12	1.14
30-40°N	35	1.00	1.42	1.14
20-30°N	135	1.00	1.40	1.11
10-20°N	123	1.01	1.55	1.10
0-10°N	124	1.00	1.43	1.10
0-10°S	243	1.00	2.09	1.15
10-20°S	315	1.01	3.57	1.12
20-30°S	316	1.00	1.44	1.13
30-40°S	206	1.01	3.81	1.14
40-50°S	125	1.04	1.44	1.15
50-60°S	96	1.04	1.44	1.15

**Table 2.** SL Lobateness Versus General Geologic Unit

	Number	Minimum $\Gamma$	Maximum $\Gamma$	Median $\Gamma$	Peak $\Gamma$ Range
Plains	399	1.00	3.33	1.10	1.0 - 1.1
Moderately Cratered Plains	281	1.00	3.34	1.12	1.1 - 1.2
Heavily Cratered	1245	1.01	3.82	1.16	1.1 - 1.2

the outermost lobe of the ML morphologies (median  $\Gamma = 1.18$ ) is consistently greater than the  $\Gamma$  of either SL craters (median  $\Gamma = 1.09$  on plains and 1.13 on highlands terrain) or the outermost lobe of DL craters (median  $\Gamma = 1.14$ ). Again, the quantitative values of lobateness vary slightly due to resolution effects, but the general trend remains: outer lobes of ML crater display higher degrees of sinuosity than the inner lobes and the lobateness of the outermost lobe of ML craters tends to be greater than the lobateness for SL craters or the outer lobe of DL craters.

Within the error limits, the lobateness for ML craters shows no correlations with either diameter or latitude (Figures 8 and 9; Table 4). Very slight variations in lobateness with general geologic unit are seen for ML craters (Table 5). But in this case, the relationship is opposite to that observed for SL craters: ML craters superposed on younger geologic units tend to display higher  $\Gamma$  values (median  $\Gamma = 1.20$ ) than those on the oldest units (median  $\Gamma = 1.17$ ), at least for the outer lobe. However, the statistical uncertainties indicate that this slight difference is not statistically significant. Finally, comparison of  $\Gamma$  with latitude-longitude, diameter-latitude, and terrain-diameter combinations reveals no correlations.

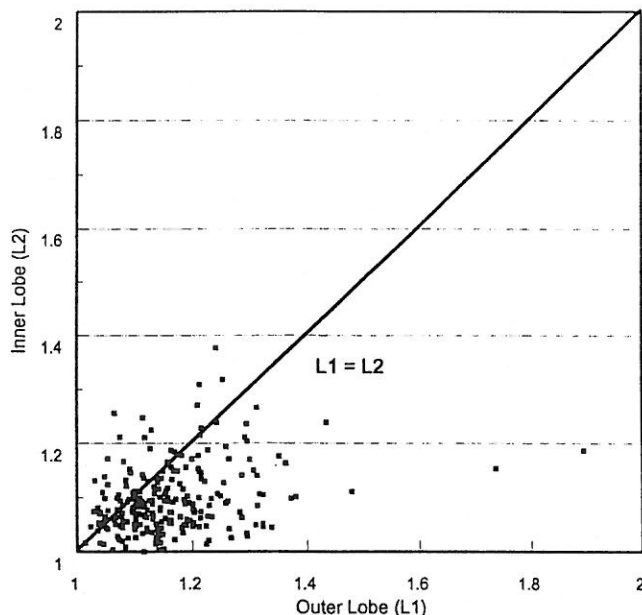


**Figure 6.** Lobateness of inner versus outer lobes of DL craters. This graph displays the measured lobateness for the inner and outer lobes of each of the 251 DL craters analyzed in this study (~130 m/pixel resolution images). The line represents a one-to-one correspondence between the two lobes. Note that the majority of points fall below this line, indicating that, for most DL craters, the inner lobe is less sinuous (i.e., lower lobateness) than the outer lobe.

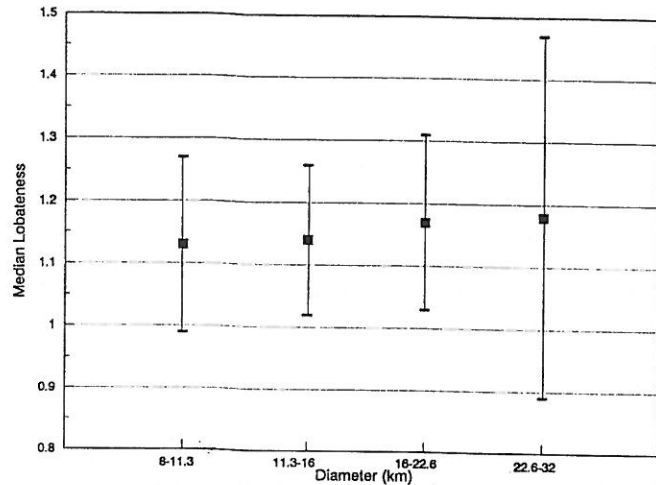


**Figure 7.** Crater diameter versus median lobateness for outer lobe of DL craters using  $\sqrt{2}$  diameter bins. Dispersion of values is  $1\sigma$  deviation. No correlation between outer lobe lobateness and crater diameter is observed. Inner lobe lobateness versus crater diameter similarly shows no correlation.

## Discussion

The lobateness results from this study are summarized in Table 6 and in general agree with the conclusions of a recent fractal study of rampart crater ejecta blankets by *Ching et al.* [1993]. However, the results reported here differ in many aspects from the conclusions of *Kargel* [1986, 1989] regarding how rampart ejecta sinuosity varies with diameter, latitude, and general geologic unit. *Kargel's* lobateness study reported an increase in  $\Gamma$  with increasing diameter, a decrease in  $\Gamma$  as one moves poleward, and a slight hemispheric asymmetry in  $\Gamma$  which may be related to geologic unit. This study finds no statistically significant correlation between  $\Gamma$  and diameter, latitude, or terrain unit. The source of the discrepancies appears to be due largely to our study of the effect of resolution on the lobateness values as well as the distinction between different ejecta morphologies. The study of ejecta morphology variation with diameter, latitude, and terrain by *Barlow and Bradley* [1990] combined with the results of the present study can explain the following of *Kargel's* conclusions:

1. *Kargel* found that lobateness was directly correlated with diameter, whereas this study finds no statistically significant cor-

**Table 3.** Summary of ML Lobateness Values

	Number	Minimum $\Gamma$	Maximum $\Gamma$	Median $\Gamma$
Outer lobe	377	1.02	1.74	1.18
Intermediate lobe	363	1.01	1.47	1.14
Inner lobe	184	1.00	1.33	1.09

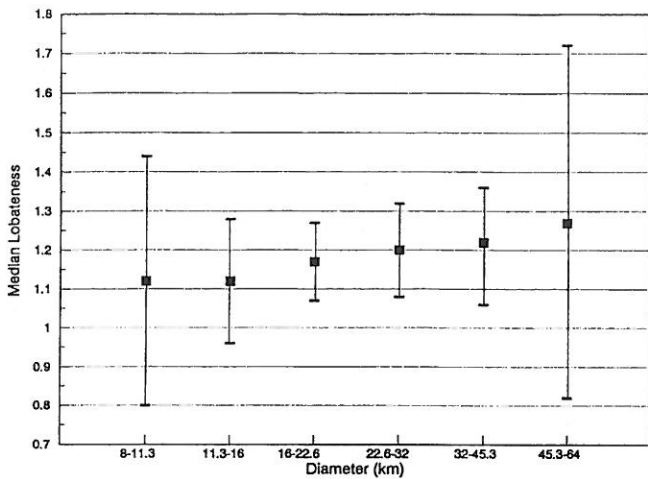


**Figure 8.** Crater diameter versus median lobateness for outer lobe of ML craters using  $\sqrt{2}$  diameter bins. No statistically significant ( $1\sigma$  level) correlation between outer lobe lobateness and crater diameter is seen. Inner and intermediate lobe lobatenesses versus crater diameter similarly show no correlation.

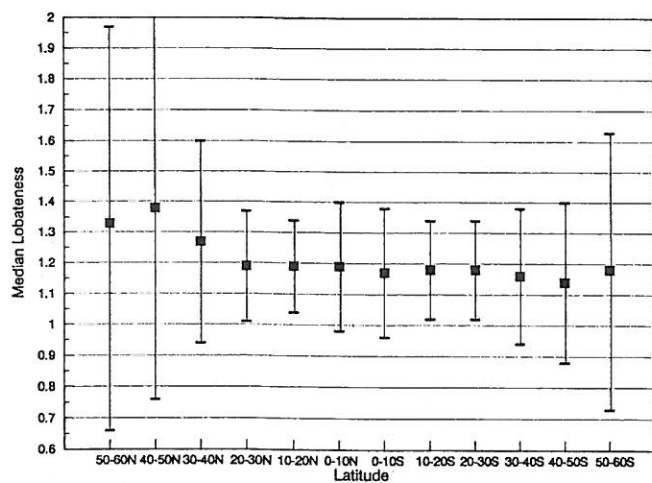


**Figure 9.** Latitude versus median lobateness for ML craters. No statistically significant ( $1\sigma$  level) latitudinal variation in lobateness is seen for the outermost lobe of ML craters.

relation between diameter and lobateness within a specific rampart morphology class. We believe this discrepancy between the two studies results from our distinction among ejecta morphologies. Barlow and Bradley found that near the equator single-lobe craters dominated at lower crater diameters (8-20 km) and multiple-lobe craters were associated with the larger craters (primarily between 15 and 45 km in diameter). This study finds that the outermost lobe of ML craters display larger  $\Gamma$  values than SL craters. If one considers all rampart craters in the equatorial region without distinguishing among the different morphologic classes, a correlation between diameter and lobateness will be reported because the smaller single-lobe craters have lower  $\Gamma$  values than the larger multiple-lobe craters.

2. Barlow and Bradley's analysis of ejecta morphology correlations with latitude revealed that at low latitudes smaller craters commonly displayed SL structures while larger craters were dominated by ML morphologies. As one moves poleward, ML morphologies decrease in number, replaced by SL morphologies which cover a larger range in diameter (up to 50-km diameter) than seen near the equator (up to 20-km diameter). Since ML

craters have larger  $\Gamma$  values than SL craters at all latitudes, ignoring the different classes of rampart ejecta morphologies would suggest that  $\Gamma$  decreases from a maximum value near the equator, exactly what Kargel reports. However, when only SL craters or only ML craters are considered, no variation in lobateness with latitude is observed.

This study also determined the variation in lobateness between the different lobes of SL, DL, and ML craters. Outer lobes of DL and ML craters tend to display higher  $\Gamma$  values than the inner lobes. These results have implications for the fluidity of the material emplaced at different stages of the impact process. Although *Mouginis-Mark* [1981] reports examples of double-lobe craters where scour marks indicate that the inner lobes were emplaced prior to the outer lobe, the majority of double-lobe and multiple-lobe craters have inner lobes superposed on the outer lobes. Impact studies also indicate that material ejected early in the crater formation process is ejected with the most energy and therefore travels further than material ejected later [Melosh, 1989]. Crater formation in a layered target is commonly cited for formation of the DL morphology [Mouginis-Mark, 1981], and can be reconciled with the results of this study if the material from which the outer lobes form have greater

**Table 4.** ML Lobateness versus Latitude

Latitude Range	Number	Minimum $\Gamma$			Maximum $\Gamma$			Median $\Gamma$		
		L1	L2	L3	L1	L2	L3	L1	L2	L3
50-60°N	4	1.10	1.13	1.06	1.38	1.44	1.33	1.33	1.21	1.21
40-50°N	5	1.13	1.20	1.12	1.47	1.41	1.12	1.38	1.25	1.11
30-40°N	15	1.12	1.07	1.08	1.64	1.38	1.22	1.27	1.23	1.14
20-30°N	42	1.02	1.04	1.05	1.61	1.47	1.25	1.19	1.14	1.09
10-20°N	64	1.05	1.01	1.01	1.45	1.44	1.18	1.19	1.13	1.07
0-10°N	31	1.06	1.06	1.08	1.59	1.42	1.26	1.19	1.14	1.12
0-10°S	30	1.08	1.05	1.05	1.46	1.27	1.20	1.17	1.15	1.13
10-20°S	52	1.07	1.03	1.03	1.42	1.37	1.28	1.18	1.13	1.10
20-30°S	55	1.06	1.04	1.01	1.51	1.35	1.22	1.18	1.13	1.10
30-40°S	28	1.09	1.05	1.01	1.41	1.28	1.21	1.16	1.11	1.08
40-50°S	20	1.04	1.02	1.01	1.23	1.37	1.16	1.14	1.14	1.08
50-60°S	7	1.12	1.04	1.06	1.38	1.30	1.18	1.18	1.09	1.08

Table 5. ML Lobateness versus General Geologic Unit

	Number	Minimum $\Gamma$	Maximum $\Gamma$	Median $\Gamma$
<i>Outer Lobe</i>				
Plains	94	1.05	1.74	1.20
Moderately Cratered Plains	58	1.07	1.51	1.20
Heavily Cratered	225	1.02	1.61	1.17
<i>Intermediate Lobe</i>				
Plains	90	1.01	1.47	1.15
Moderately Cratered Plains	55	1.04	1.35	1.15
Heavily Cratered	218	1.02	1.41	1.13
<i>Inner Lobe</i>				
Plains	35	1.01	1.33	1.10
Moderately Cratered Plains	33	1.01	1.26	1.10
Heavily Cratered	116	1.00	1.28	1.09

Table 6. General Results of Lobateness Study

	SL		DL		ML		
	Plains	Highlands	L1	L2	L1	L2	L3
Number	370	1212	251	245	380	363	184
Median $\Gamma$	1.09	1.13	1.14	1.09	1.18	1.13	1.09
Maximum $\Gamma$	3.33	3.81	2.27	1.38	1.74	1.47	1.33
Minimum $\Gamma$	1.00	1.01	1.01	1.00	1.02	1.10	1.00

fluidity (larger volatile/clast ratio) than the material from which the inner lobes form. If the outer lobe of a DL ejecta morphology forms prior to emplacement of the inner lobe, this implies that volatile content is greater in the near-surface layer. Although the general view of the Martian substrate is one where more desiccated layers are in contact with the atmosphere and more volatile-rich layers lie at greater depths, most DL craters are located in the high latitude zones where ice-rich soil is stable in contact with the atmosphere [Fanale, 1976; Paige, 1992; Mellon and Jakosky, 1993]. Therefore, a layered target with higher volatile/clast ratio in the upper layer can exist and be stable, thus explaining how a more sinuous outer lobe can be emplaced before the less sinuous (i.e., "drier") inner lobe.

The multilobate structure of ML craters is attributed to vapor surges caused by changes in the ratio of vapor to clast volume, reflecting the changing amount of vapor produced by impact into water versus ice [Wohletz and Sheridan, 1983]. The higher sinuosity of ML craters is predicted by this model because of this higher vapor to clast volume ratio.

Taken alone, the results of this quantitative study of rampart ejecta sinuosity can be satisfied by either the subsurface volatile [Carr et al., 1977] or the atmospheric [Schultz and Gault, 1979; Schultz, 1992] formation theories. This study finds that ML craters, which tend to be associated with larger craters, tend to display higher  $\Gamma$  values than the smaller SL and DL morphologies. The subsurface volatile model proposes that multiple-lobe morphologies would be more sinuous than single-lobe morphologies because ML craters form by impact into less viscous materials. The atmosphere model proposes that more energetic impact events will produce multiple-lobes of higher sinuosity than smaller, less energetic events. However, in concert with

the results of the Barlow and Bradley [1990] study of the distribution of ejecta morphologies and their correlations with diameter, latitude, and (to a lesser extent) geologic unit, the evidence is strongly supportive of the theory that lobate ejecta morphologies result from impact into and vaporization of subsurface volatiles.

**Acknowledgments.** The author wishes to thank Nathan Bridges for his assistance in the collection of SL and DL lobateness data and for comments on this manuscript. Helpful reviews were provided by Barbara Bruno and Jeffrey Kargel. This research was conducted in part while the author was a Visiting Post Doctoral Fellow at the Lunar and Planetary Institute, which is operated by the Universities Space Research Association under contract NASW-4066 with the National Aeronautics and Space Administration. Lunar and Planetary Institute Contribution 830.

## References

- Baker, V. R., V. C. Gulick, and J. S. Kargel, Water resources and hydrogeology of Mars, in *Resources of Near-Earth Space*, edited by J. S. Lewis, M. S. Matthews, and M. L. Guerrieri, pp. 765-797, University of Arizona Press, Tucson, 1993.
- Barlow, N. G., Crater size-frequency distributions and a revised Martian relative chronology, *Icarus*, 75, 285-305, 1988.
- Barlow, N. G., and T. L. Bradley, Martian impact craters: Correlations of ejecta and interior morphologies with diameter, latitude, and terrain, *Icarus*, 87, 156-179, 1990.
- Blasius, K. R., and J. A. Cutts, *Planetary geologic studies final report*, NASA contract NASW-3208, 1981.
- Carr, M. H., L. S. Crumpler, J. A. Cutts, R. Greeley, J. E. Guest, and H. Masursky, Martian impact craters and emplacement of ejecta by surface flow, *J. Geophys. Res.*, 82, 4055-4065, 1977.
- Ching D., G. J. Taylor, P. Mouginiis-Mark, and B. C. Bruno, Fractal



- dimensions of rampart impact craters on Mars (abstract), *Lunar Planet. Sci. Conf.*, XXIV, 283-284, 1993.
- Costard, F. M., The spatial distribution of volatiles in the Martian hydrolithosphere, *Earth Moon Planets*, 45, 265-290, 1989.
- Crater Analysis Techniques Working Group, *Standard techniques for presentation and analysis of crater size-frequency data*, NASA Tech. Memo., 79730, 1978.
- Fanale, F. P., Martian volatiles: Their degassing history and geochemical fate, *Icarus*, 28, 179-202, 1976.
- Gault, D. E., and R. Greeley, Exploratory experiments of impact craters formed in viscous-liquid targets: Analogs for Martian rampart craters?, *Icarus*, 34, 486-495, 1978.
- Greeley, R., J. Fink, D. E. Gault, D. B. Snyder, J. E. Guest, and P. H. Schultz, Impact cratering in viscous targets: Laboratory experiments, *Proc. Lunar Planet. Sci. Conf.*, 11th, 2075-2097, 1980.
- Horner, V. M. and R. Greeley, Effects of elevation and ridged plains thickness on Martian crater ejecta morphology, *Proc. Lunar Planet. Sci. Conf. 17th, Part 2*, *J. Geophys. Res.*, 92, suppl., E561-E569, 1987.
- Johansen, L. A., Martian splash cratering and its relation to water (abstract), *Proc. 2nd Colloquium on Planetary Water and Polar Processes*, pp. 109-110, U.S. Army Cold Regions Research and Engineering Laboratory, Hanover, N.H., 1978.
- Johansen, L. A., The latitude dependence of Martian splash cratering and its relationship to water, *Report of the Planetary Geology Program 1978-1979*, NASA Tech. Memo., 80339, 123-125, 1979.
- Kargel, J. S., Morphologic variations of Martian rampart crater ejecta and their dependencies and implications (abstract), *Lunar Planet. Sci.*, XVII, 410-411, 1986.
- Kargel, J. S., First and second-order equatorial symmetry of Martian rampart crater ejecta morphologies (abstract), *Fourth International Conference on Mars*, pp. 132-133, University of Arizona, Tucson, 1989.
- Kieffer, S. W., and C. H. Simond, The role of volatiles and lithology in the impact cratering process, *Rev. Geophys.*, 18, 143-181, 1980.
- Mellon, M. T., and B. M. Jakosky, Geographic variations in the thermal and diffusive stability of ground ice on Mars, *J. Geophys. Res.*, 98, 3345-3364, 1993.
- Melosh, H. J., *Impact Cratering: A Geologic Process*, Oxford University Press, New York, 1989.
- Mouginis-Mark, P., Martian fluidized crater morphology: Variations with crater size, latitude, altitude, and target material, *J. Geophys. Res.*, 84, 8011-8022, 1979.
- Mouginis-Mark, P., Ejecta emplacement and modes of formation of Martian fluidized ejecta craters, *Icarus*, 45, 60-76, 1981.
- Neukum, G., and K. Hiller, Martian ages, *J. Geophys. Res.*, 86, 3097-3121, 1981.
- Paige, D.A., The thermal stability of near-surface ground ice on Mars, *Nature*, 356, 43-45, 1992.
- Schultz, P. H., Atmospheric effects on ejecta emplacement, *J. Geophys. Res.*, 97, 11,623-11,662, 1992.
- Schultz, P. H., and D. E. Gault, Atmospheric effects on Martian ejecta emplacement, *J. Geophys. Res.*, 84, 7669-7687, 1979.
- Schultz, P. H., and D. E. Gault, Impact ejecta dynamics in an atmosphere: Experimental results (abstract), *Lunar Planet. Sci.*, XIII, 696-697, 1982.
- Schultz, P. H., and D. E. Gault, On the formation of contiguous ramparts around Martian impact craters (abstract), *Lunar Planet. Sci.*, XV, 732-733, 1984.
- Tanaka, K. L., The stratigraphy of Mars, *Proc. Lunar Planet. Sci. Conf.*, 17th, Part 1, *J. Geophys. Res.*, 91, suppl., E139-E158, 1986.
- Wohletz, K. H., and M. F. Sheridan, Martian rampart crater ejecta: Experiments and analysis of melt-water interactions, *Icarus*, 56, 15-37, 1983.

N. G. Barlow, Lunar and Planetary Institute, 3600 Bay Area Boulevard, Houston, TX 77058. (e-mail: Barlow@lpi.jsc.nasa.gov)

(Received June 17, 1993; revised March 4, 1994; accepted March 8, 1994.)